Journal of The Electrochemical Society, **146** (5) 1640-1642 (1999)
S0013-4651(98)08-030-6 CCC: $7.00

Improving the Electrochemical Performance of SnO_2 Cathodes in Lithium Secondary Batteries by Doping with Mo

Julián Morales*,z and Luis Sánchez

Laboratorio de Química Inorgánica, Facultad de Ciencias, Universidad de Córdoba, E-14004 Córdoba, Spain

Small-grain SnO_2, SnO_2/Mo (2%), and SnO_2/Mo (30%) samples were prepared by using low-temperature aqueous methods and tested as cathodes in secondary lithium batteries. Cells were cycled between 1.0 and 0.0 V. The best electrochemical performance was obtained from the Li/[SnO_2/Mo (2%)] cell, which retained 87% of its initial capacity (510 mAh/g) after 50 cycles; by contrast, the Li/SnO_2 cell only retained 60% of its initial capacity (570 mAh/g). Significantly increased Mo contents caused the capacity to fade drastically.

Manuscript submitted August 10, 1998; revised manuscript received November 13, 1998.

Rechargeable lithium batteries are now available as competitive energy sources as a result of intensive research into lithium compounds. Safety and rechargeability problems associated to the use of metallic lithium have so far prevented widespread marketing, however. Several authors[1] have proposed the use of another intercalation compound as the anode to make the so-called "rocking chair" or "lithium ion" batteries. These systems were first commercialized by Sony Energetics Inc., in 1990, with carbon as anode. This was the result of interesting research activity on negative electrode materials other than lithium metal.

Recently, a new family of compounds based on SnO composites was tested for use as anodes in lithium ion cells.[2] These insertion electrodes can incorporate about 6 mol of Li per tin atom, which corresponds to 1030 mAh/g. Although the initial discharge efficiency decreases by 37%, a reversible Li-ion storage capacity above 600 mAh/g (twice as high as in carbon-based anodes) is maintained. These findings have aroused the interest of several groups in testing the ability of SnO_2, an n-type semiconductor commonly used in conductimetric sensors, to act as an insertion electrode in lithium cells.[3-6] Although these investigation have shed light on some aspects of the structural changes in SnO_2 upon lithium insertion, and also on some factors controlling the reversibility of the reaction, significant capacity fading upon cycling has been observed.[3] In this respect, its worth mentioning the report of Krasovec et al.[7] on the favorable effect of doping SnO_2 with Mo, which improves its electrochromic and electrochemical properties. In our opinion, such interesting behavior may open promising new prospects for improving of electrochemical performance of SnO_2 as insertion electrode in lithium cells.

This paper describes the preparation and characterization of small-grain tin oxides doped with different amounts of Mo, as well as the investigations carried out in order to study the influence of this new dopant element on the structural and electrochemical properties of SnO_2 and its implications on the cell capacity retention on cycling.

Experimental

Pure microcrystalline SnO_2 was prepared by a hydrothermal procedure starting from a 0.25 M solution of $SnCl_4 \cdot 5H_2O$ in 8 N nitric acid.[8] The solution was heated in a Teflon-lined stainless tank at 150°C for 14 h, and then cooled to room temperature to obtain a white powder. Doped tin oxides, which were prepared in Mo contents of 2 and 30% relative to total metal, were obtained by dropwise addition of 30 weight percent (wt %) H_2O_2 (15 mL) to 7 g of $SnCl_4 \cdot 5H_2O$, followed by mixing with an appropriate amount of Mo metal powder and heating at 60°C until a white powder was formed.[7] In both processes, the precipitates were washed several times to remove residual NO_3^- and Cl^- ions. The final stoichiometry of the precipitates was determined by atomic absorption spectrometry. X-ray diffraction (XRD) patterns were recorded on a Siemens D5000 X-ray diffractometer, using Cu Kα radiation and a graphite monochromator.

Electrochemical experiments were carried out in two-electrode cells, using lithium as the anode. The electrolyte used was 1 M anhydrous $LiPF_6$ in a 1:1 mixture of ethylene carbonate (EC) and dimethyl carbonate (DMC). Oxide electrode pellets (7 mm diam) were prepared by pressing ca. 4 mg of active material with polytetrafluoroethylene (PTFE) (5 wt %), graphite (7.5 wt %), and acetylene black (7.5 wt %) at 4 tons. Lithium foil was cut as 7 mm circles of diameter. Unless otherwise noted, cells were cycled at a 0.25 mA/cm^2 current density, controlled via a MacPile II potentiostat-galvanostat.

Results and Discussion

Figure 1 shows the XRD spectra for the three samples studied. The spectrum for the undoped sample coincides with that for the tetragonal phase of SnO_2, with no additional lines belonging to other phases such as SnO. Two significant features warrant some comment. First, the diffraction peaks are markedly broadened, consistent with low crystallinity in the particles. Second, the diffraction lines are anisotropically broadened. The lines with a non-zero *l* component are narrower than the other peaks. This suggests that the crystals tend to growth along the *z* direction and prevents application of

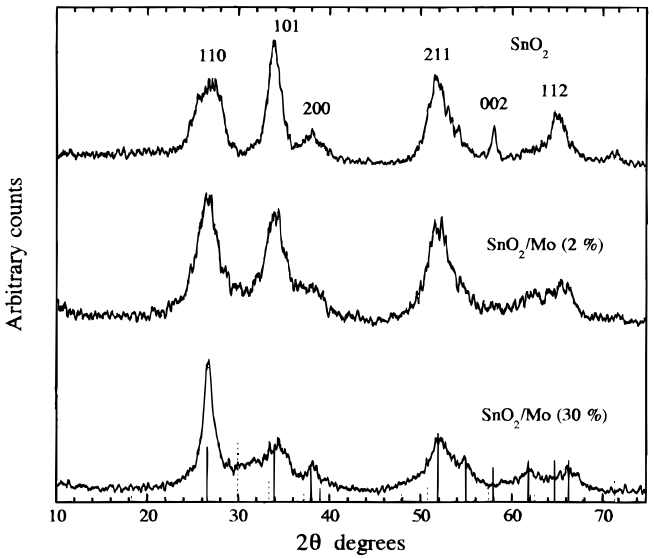

Figure 1. Powder X-ray diffraction patterns for the SnO_2 and SnO_2/Mo oxides. [(—): SnO_2 JCPDS pattern; (-----): SnO JCPDS pattern].

* Electrochemical Society Active Member.
z E-mail: ig1mopaj@uco.es

S0013-4651(98)08-030-6 CCC: $7.00

Table I. Unit cell parameters and crystallite size of SnO_2 and SnO_2/Mo samples.

Sample	*a* (Å)	*c* (Å)	*V* (Å^3)	*L* (Å) 110	*L* (Å) 101	*L* (Å) 211
SnO_2	4.73(1)	3.171(5)	70.9	27	61	57
SnO_2/Mo (2%)	4.73(1)	3.15(1)	70.5	69	—	—
SnO_2/Mo (30%)	4.73(2)	3.119(6)	69.8	40	48	48

a broadening analysis methods such as those of the integral breath type to discriminate the contribution of crystallite size and microstrain content to line broadening. For this reason, we used the Scherrer equation to calculate the crystallite sizes given in Table I. As can be seen, reflections with $l \neq 0$ lead to similar crystallite sizes that are twice as large as those for reflections with a zero *l* component. The XRD patterns for Mo doped samples (Fig. 1) are also indicative of poorly crystallized samples and exhibit no diffraction peaks corresponding to any high-oxidation state Mo phase (e.g., $MoO_3 \cdot H_2O$). One salient feature of the sample with a low Mo content is the loss of preferential broadening in the peaks (*hk0*). Crystallite size is now essentially independent of the reflection used and somewhat smaller than for the undoped sample. Moreover, the increased Mo content seems to affect the relative intensities of the peaks, the (*110*) reflection is stronger and sharper. These findings suggest that Mo affects the habit growth of the crystallites and facilitates growing along the [*hk0*] direction.

On the other hand, the unit cell parameters collected in Table I, showed a weak decrease as the Mo content was increased. This is consistent with the small ionic radius of Mo^{6+} (0.62 Å) relative to Sn^{4+} (0.71 Å), and also with the finding of Krasovec et al.[7] that no aggregation of Mo species occurs at similar Mo contents. Moreover, the IR spectra are coincident with those reported for SnO_2/Mo films.[7] The appearance of three bands at 942, 863, and 806 cm^{-1} associated with Mo-O stretching modes is indicative of Mo ions in octahedral coordination probably located in the cassiterite structure in a random distribution. In any case, acquiring an accurate knowledge of the actual environment of Mo would have required complementary structural studies that were beyond the scope of this communication.

Figure 2 shows the first discharge curve for the Li/SnO_2 cell, recorded at a current density of 0.25 mAh/g. The curve shape is similar to that reported by Courtney and Dahn[3] for a commercial SnO_2 sample and by Liu et al.[6] for an SnO_2 sample prepared by hydrolysis of $SnCl_4 \cdot 5H_2O$ and heating at 300°C for 4 h. The two pseudo plateaux in the discharge curve can be interpreted in the light of the arguments given by these authors, viz. the initial formation of Sn, followed by

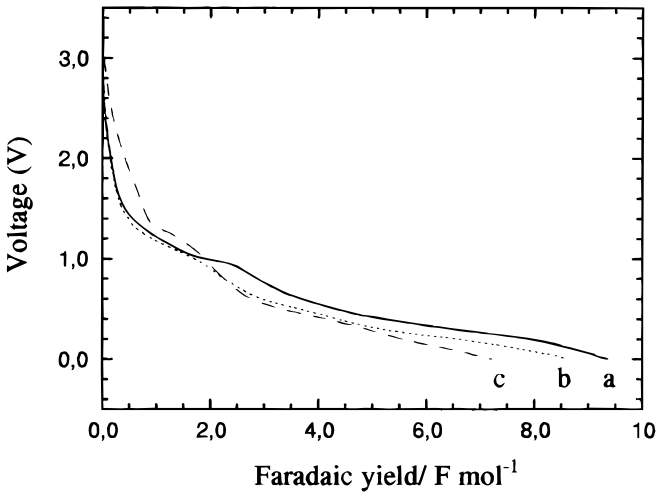

Figure 2. Galvanostatic discharge curves for (a) Li/SnO_2, (b) Li/[SnO_2/Mo (2%)], and (c) Li/[SnO_2/Mo (30%)] cells.

that of an Li_ySn alloy. Doping with Mo mainly affects the plateau at about 1.0 V, which becomes shorter and less ostensible. Moreover, the total capacity decreases as the Mo content increases.

Before the cycling behavior of the samples was studied, preliminary tests were carried out on the Li/SnO_2 cell in order to select the optimum working voltage limits. These voltage windows can influence the size of the tin regions and apparently cause aggregation of the tin as a function of the number of cycles, thus causing the cell capacity to fade.[4] The limits 1.0 - 0.0 V were found to form the best voltage window where the capacity loss was minimal. Under these conditions, a specific capacity of 570 mAh/g was obtained in the first charge process.

Plots of differential specific capacities are useful tools for analyzing the reversibility of an electrochemical oxidation-reduction process. Unchanged profiles of the derivatives curves on cycling indicate a reversible lithium extraction-insertion process.[4] Figure 3 shows the *dq*/(*mdv*) vs. voltage plots for the first, third, and fifth charge-discharge sequence of Li/LPF_6 (EC-DMC)/SnO_2 and Li/LPF_6 (EC-DMC)/(SnO_2/Mo) cells between 0.0 and 1.0 V. These voltage-capacity profiles correspond to the lower voltage plateau where the Li_ySn alloys are formed. With the SnO_2 and SnO_2/Mo (2%) samples, the reversibility of the oxidation-reduction process is apparent from the symmetric anodic and cathodic waves obtained (see Fig. 3). However, the differential capacity curves for the SnO_2/Mo (30%) sample behave differently. The peaks are less well defined and the fact that the forward and reverse curves are differently shaped suggests that the oxidation-reduction process tends to be irreversible.

The specific capacity of the cells made from the three samples, cycled between 0.0 and 1.0 V, is shown as a function of the number of cycles in Fig. 4. For comparison, this figure also shows the results obtained for a cathode made of graphite, acetylene black, and PTFE (1.5:1.5:1 ratio, respectively), since these carbons can intercalate lithium in the potential window used. The specific capacity of this cell markedly drops and after a few cycles the value is lower than 30 Ah/kg. This means that the active material is responsible for the cell performance. As can be seen in Fig. 4, the presence of Mo influences the cell retention capacity. The cycling properties of SnO_2 resemble those observed by Courtney and Dahn[4] in SnO_2 prepared by thermal decomposition of Sn(IV) acetate at 390°C on cycling between 0.0 and 0.8 V. In fact, its crystallite size is comparable to that in Table I. This undoped sample exhibited the highest capacities in the first few charge-discharge cycles, which, however, decreased significantly after the fifteenth cycle. A drastic capacity drop was the dominant feature of cell made from the SnO_2/Mo (30%) sample, a result of the peculiar characteristics of the above-described differential capacity curves. The best results were obtained with the Li/[SnO_2/Mo (2%)] cell, which in spite of a moderately decreased capacity relative to SnO_2 in the first few cycles, retained 87% after the first 50 cycles (Fig. 4). By contrast, the cell made from the undoped sample retained only 60% of the initial capacity.

These results are reasonably consistent with the finding of Krasovec et al.[7] that the presence of Mo in SnO_2 increases electrochemical reversibility. In our case, doping SnO_2 with small amounts of Mo clearly improved the cycling performance of the Li cell. We believe that it is the result of at least two factors. First, Mo definitely influences growth of the coherent diffracting domain, as shown by the line broadening observed. Second, the presence of Mo in the Li-Sn alloy formed may favor Sn atom dispersion, a key to the reversibility of Li reaction. In this context, the appearance of peaks in the differen-

S0013-4651(98)08-030-6 CCC: $7.00

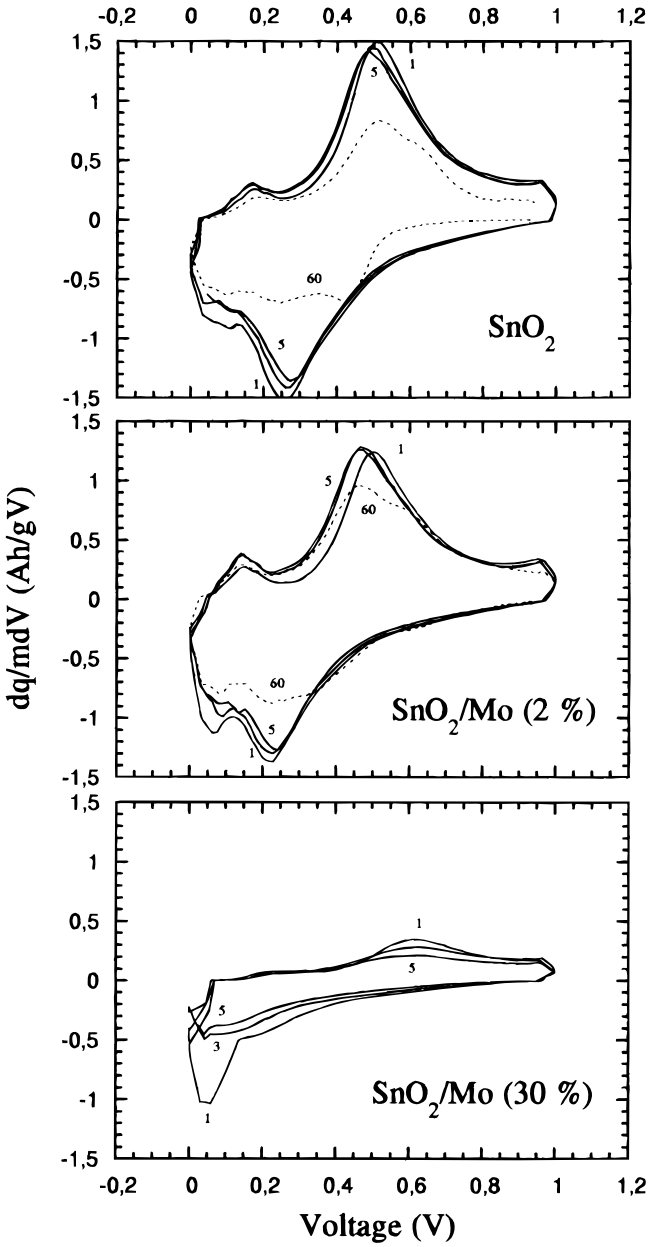

Figure 3. Derivative voltage curves (V vs. Ah/gV) for SnO_2 and SnO_2/Mo oxides cycled between 0.0 and 1.0 V.

tial capacity curves have been associated with the formation of Sn clusters of significant dimensions.[4] Such behavior is indeed observed for the SnO_2 sample, the differential capacity of which shows the growth of a peak located around 0.4 V as the cycle number increases. In contrast, this peak is absent in the Mo-doped sample. At high Mo contents, the Li-Sn-Mo alloy formed, for reasons still unclear, decreases the reversibility of lithium insertion-extraction. Research currently in progress is being made to optimize the Mo content for improved the cell capacity retention, and also to acquire an accurate picture of the structural and electronic properties of Mo through a better understanding of its role in the electrochemical reaction.

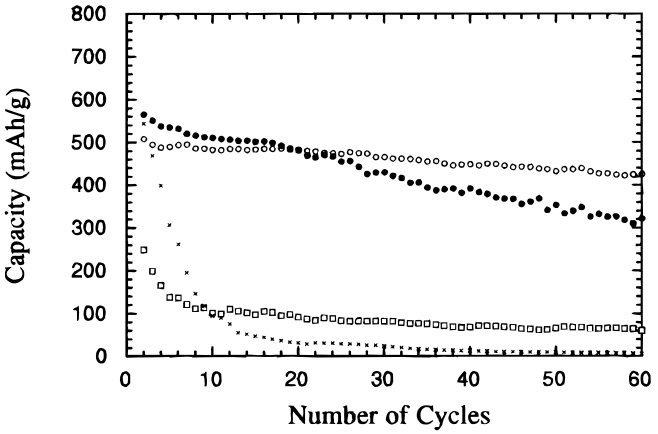

Figure 4. Delivered cathode capacity from galvanostatic cycling of (●) Li/SnO_2, (○) Li/[SnO_2/Mo (2%)], (□) Li/[SnO_2/Mo (30%)], and (x) Li/[graphite-acetylene black-PTFE] cells.

Conclusions

Doping SnO_2 with a small amount of Mo improves its electrochemical cycling performance as cathode material for secondary lithium batteries operating in the 1.0-0.0 V voltage range. However, the presence of a significant amount of Mo in the oxide has an adverse effect on its cycling properties. Differences in crystallite growth, and easier dispersion of Sn atoms formed during the reduction process, are two plausible origins for the enhancing effect of the transition metal.

Acknowledgments

The work was supported by Spain's Ministerio de Educación y Cultura (CICYT Project PB95-0561) and the Junta de Andalucía (Group FQM-175).

Universidad de Córdoba assisted in meeting the publication costs of this article.

References

1. M. Lazari and B. Scrosati, *J. Electrochem. Soc.*, **127,** 773 (1980).
2. Y. Idota, T. Kubota, A. Matsufuji, Y. Maekawa, and T. Miyasaka, *Science*, **276,** 1395 (1997).
3. I. A. Courtney and J. R. Dahn, *J. Electrochem. Soc.*, **144,** 2045 (1997).
4. I. A. Courtney and J. R. Dahn, *J. Electrochem. Soc.*, **144,** 2943 (1997).
5. T. Brousse, R. Retoux, U. Herterich, and D. M. Schleich, *J. Electrochem. Soc.*, **145,** 1 (1998).
6. W. Liu, X. Huang, Z. Wang, H. Li, and L. Chen, *J. Electrochem. Soc.*, **145,** 59 (1998).
7. U. O. Krasovec, B. Orel, S. Hocevar, and Y. Musevic, *J. Electrochem Soc.*, **144,** 3398 (1997).
8. K. N. Yu, Y. Xiong, Y. Liu, and C., *Phys. Rev. B*, 2666 (1997).